

are more nearly equivalent in the mass spectra of  $B_8H_{18}$  and the tetraboranes. Formation of  $B_4H_8$  as well as  $B_4H_{10}$  is suggested by the fact that the absolute intensity of  $m/e$  48 remained constant while that of  $m/e$  50 decreased. The behavior of  $I(53^+)$  relative to  $I(52^+)$  (Figure 3) can be explained by the formation of tetraborane(8) and tetraborane(10) both of which would contribute more ion intensity to  $m/e$  52 than to  $m/e$  53 and cause a relative decrease of  $I(53^+)$ . At high temperatures, pentaborane is formed and would contribute more ion intensity to  $m/e$  53 than to  $m/e$  52 causing the observed increase in the ratio  $I(53^+)/I(52^+)$ .

Although the ratios  $I(37^+)/I(52^+)$  and  $I(27^+)/I(52^+)$  increase with increasing temperature, formation of di- or triboranes is not necessarily indicated. Even though the absolute intensities of these peaks increase between approximately 130 and 170°, relative intensity changes for these two peaks are considerably less than that for the tetraboranes. Fragmentation of the  $B_4H_8$ ,  $B_4H_{10}$ ,  $B_5H_9$ , and the hexaborane, all of which are believed to be formed, could account for the observed increases.

## Conclusions

The unusual fragmentation pattern in the molecular beam mass spectrum of octaborane(18) is strong evidence for a structure in which two  $B_4H_8$  groups are joined by a single B-B bond. An appearance potential of  $11.2 \pm 0.1$  eV determined for  $B_4H_8^+$  also supports this structure.

Pyrolysis of octaborane(18) appears to lead to tetraborane(8) and tetraborane(10). Formation of pentaborane(9), possibly pentaborane(11), and hexaborane(s) is indicated; however, their formation may result from the pyrolysis of the tetraboranes. Increase with temperature of diborane and triborane ion intensities is observed but can be due to fragmentation of other pyrolysis products.

This work shows also that comparison of the molecular beam and total intensity mass spectra can help identify the pyrolysis products of a boron hydride. The conclusions drawn from such a comparison and the pyrolysis study are in agreement for octaborane(18).

CONTRIBUTION FROM THE DEPARTMENT OF CHEMISTRY  
AND LAWRENCE RADIATION LABORATORY, UNIVERSITY OF CALIFORNIA, BERKELEY, CALIFORNIA 94720

## The Crystal and Molecular Structure of Phosphorus Trifluoride-Tris(difluoroboryl)borane, $B_4F_6 \cdot PF_3$ <sup>1</sup>

BY BARRY G. DEBOER,<sup>2</sup> ALLAN ZALKIN, AND DAVID H. TEMPLETON

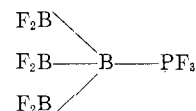
Received September 6, 1968

The crystal structure of phosphorus trifluoride-tris(difluoroboryl)borane,  $B_4F_6 \cdot PF_3$ , has been determined by an X-ray diffraction study of single-crystal specimens. The orthorhombic unit cell, space group  $Pnma$ , with  $a = 13.893 \pm 0.005$  Å,  $b = 10.578 \pm 0.005$  Å, and  $c = 6.075 \pm 0.005$  Å, contains four formula units. The calculated density is 1.82 g/cm<sup>3</sup>. The structure was solved by statistical methods and refined by full-matrix least squares to a conventional  $R$  of 9.3% for 703 data collected by counter methods (6.7% for the 603 nonzero data). The molecule consists of a central boron atom, tetrahedrally bonded to three  $BF_2$  groups and the  $PF_3$  group in such a way that the molecule has approximately 3m ( $C_{3v}$ ) point symmetry, one mirror of which is required by the crystal symmetry. Distances found (uncorrected for thermal motion) are: B-F, 1.305 Å; B-B, 1.68 Å; B-P, 1.825 Å; P-F, 1.51 Å (all  $\pm 0.015$  Å).

### Introduction

Timms has recently reported<sup>3</sup> the synthesis of a number of novel boron fluoride compounds by reactions of the high-temperature species, boron monofluoride, on cold surfaces. Cocondensation of  $BF_3$  and  $PF_3$  produces  $B_4F_6 \cdot PF_3$ , a pyrophoric and water-sensitive substance which readily sublimes (mp 55°, bp 74°) to form well-developed, colorless crystals which are stable at room temperature. The present X-ray diffraction

investigation was undertaken to verify the proposed structure



and to determine the bond distances and angles in this molecule.

### Experimental Section

Samples of the compound, sealed into thin-walled glass capillaries, were provided by Professor Timms. Crystals formed quite readily as the compound was sublimed back and forth in the

(1) Work done under the auspices of the U.S. Atomic Energy Commission.

(2) National Science Foundation graduate fellow, 1964-1967.

(3) P. L. Timms, *J. Am. Chem. Soc.*, **89**, 1629 (1967).

capillaries under the very mild heating provided by a beam of light from a low-voltage lamp. Persistence seemed to be the only way to obtain a suitable crystal which did not have others nearby. Complete data sets were taken on two different crystals.

The first crystal was a plate about  $0.16 \times 0.51 \times 2.2$  mm, where the intermediate dimension is the inside diameter of its capillary. A crystal this large was accepted because there was no assurance of ever obtaining a better one and because of the low absorption coefficient,  $\mu$ , of  $4.3 \text{ cm}^{-1}$  for Mo  $K\alpha$  radiation. The crystal was mounted with its long dimension,  $b$  axis, and capillary parallel to the instrument  $\varphi$  axis. Preliminary oscillation and Weissenberg photographs gave the extinction rules, Laue symmetry, and rough cell dimensions. More accurate cell dimensions were derived from the Bragg angles of the  $h00$ ,  $0k0$ , and  $00l$  reflections measured with a General Electric manual goniostat using molybdenum radiation and a Zr filter at the receiving slit. The components of the  $\alpha$  doublet were resolved ( $\lambda(\text{Mo } K\alpha_1) 0.70926 \text{ \AA}$ ) at the highest angles, but the peaks were broad and the positions of reflections at low  $\chi$  angles could not be accounted for except by assuming a  $2\theta$  correction as a function of  $\varphi$ . It is suspected that these difficulties were caused by the large size of the crystal, which was certainly longer and probably wider than the beam diameter, and by strains in the crystal (see below). In spite of these troubles, a one-octant data set of 830 independent intensities, exclusive of space group absences, was taken, using the same apparatus, by counting each reflection for 10 sec with crystal and counter stationary methods and an approximately  $3.5^\circ$  takeoff angle to the X-ray tube anode. Of these, 173 were recorded as zero. Measurements were also made at all of the locations in the region of the data set which correspond to space group absences. They were found to confirm the extinction rules of  $0kl$ ,  $k+l \neq 2n$ , and  $hk0$ ,  $h \neq 2n$ . Individual backgrounds were measured for those reflections which were seriously affected by streaking from other orders; otherwise, backgrounds were taken from a plot of background as a function of  $2\theta$  at various values of  $\varphi$  and  $\chi$ . Three standard reflections which were measured at frequent intervals during the course of data taking showed only small, random fluctuations. Measurements included reflections up to  $2\theta = 50^\circ$  ( $(\sin \theta)/\lambda = 0.595$ ). Standard deviations were assigned to the measurements of 5% of the intensity or a fixed minimum (8, 5, or 3 counts/sec, for low, intermediate, and high  $2\theta$ ), whichever was greater. The structure was initially solved using this data set, which was then definitely seen to be of unacceptable quality. A second set of samples was provided by Professor Timms, and a better crystal was sought.

The second crystal had the shape of a cylinder  $\sim 0.14$  mm long and  $\sim 0.15$  mm in diameter (the inside diameter of its capillary). Nickel-filtered copper radiation was used in order to obtain as large a data set as possible from this smaller crystal. The smaller size of this crystal made the larger absorption coefficient,  $\mu$ , of  $39 \text{ cm}^{-1}$  for Cu  $K\alpha$  radiation acceptable. The maximum variation in transmission factors is estimated to be less than 20%. The crystal was mounted with its cylinder axis,  $a$ , and capillary parallel to the instrument  $\varphi$  axis. The cell dimensions were determined as before, and found to predict correctly the position of off-axis reflections, in contrast to the trouble experienced with the first crystal. When a narrow receiving slit was being used to obtain accurate cell dimensions, the peaks were sharp and well formed and the  $\alpha$  doublet ( $\lambda(\text{Cu } K\alpha_1) 1.5405 \text{ \AA}$ ) was resolved in a majority of cases. After the slit was removed, the peaks at low  $\chi$  angles showed a characteristic broad shape with an irregular top in both  $2\theta$  and  $\omega$  scans. At high  $\chi$  angles, a narrower, regular peak shape was maintained. This is again ascribed to distortions in the crystal, since the troubles with the two crystals (this and the previous one) seem to be correlated with the direction of the capillary axis and not with the directions of the crystallographic axes. The strains might have been the result of growth on a curved surface or of slight flexings of the thin-walled capillaries as they were handled. However, it was found

that the calculated settings reproducibly gave the same part of the irregular peaks (and the tops of the regular ones) and that point counts taken at the calculated settings on a few peaks at  $\chi = 0$  and  $90^\circ$  were in the same ratio as the integrated counts obtained by scanning through those peaks (in  $2\theta$ ). A second data set of 703 intensities, including 100 recorded as zero, but not including space group absences, was taken in the same way as before. Backgrounds were likewise obtained as before, and, again, frequently measured standard reflections showed no systematic variations. The maximum value of  $2\theta$  was  $120^\circ$  ( $(\sin \theta)/\lambda = 0.562$ ). A standard deviation of 2.25 counts/sec or 7.5% of the intensity, whichever was greater, was assigned to each measurement. Both data sets were corrected for Lorentz and polarization effects, but no corrections were made for absorption or extinction.

All computations were performed on a CDC 6600 instrument. Zalkin's unpublished FORDAF and DISTAN programs were used for Fourier syntheses and distance and angle calculations, while an unpublished Wilson-plot program by Maddox and Maddox gave normalized structure factor magnitudes<sup>4</sup> which were used in Long's sign-determining program<sup>5</sup> as described below. The unpublished version of the Gantzel-Sparks-Trueblood least-squares program which was used minimizes the function  $\sum w(|kF_o| - |F_c|)^2 / \sum w|kF_o|^2$ , where  $F_o$  and  $F_c$  are the observed and calculated structure factors,  $k$  is the scale factor, and  $w$  is the weighting factor. For the early refinements, scattering factors for neutral phosphorus, fluorine, and boron were taken from standard tables.<sup>6</sup> The phosphorus scattering factors were corrected for the real part of anomalous dispersion by  $+0.1 e^-$  for the molybdenum data and  $+0.2 e^-$  for the copper data, and the imaginary part was neglected. The final refinements were performed using the scattering factors listed by Cromer and Waber<sup>7</sup> and both real and imaginary anomalous dispersion corrections given by Cromer.<sup>8,9</sup> The anisotropic temperature factors used have the form:  $\exp(-0.25 \sum_i h_i h_j b_i b_j B_{ij})$ ,  $i, j = 1, 2, 3$ , where  $b_i$  is the  $i$ th reciprocal cell length.

## Results

Four formula units of  $(\text{BF}_2)_3\text{B} \cdot \text{PF}_3$  are contained in the orthorhombic unit cell, space group Pnma, with  $a = 13.893 \pm 0.005 \text{ \AA}$ ,  $b = 10.578 \pm 0.005 \text{ \AA}$ , and  $c = 6.075 \pm 0.005 \text{ \AA}$ . The calculated density is  $1.82 \text{ g/cm}^3$ . No direct measurement of the density was attempted because of the highly reactive nature of the compound. The Laue symmetry and observed extinction rules correspond to space groups Pnma and Pn2<sub>1</sub>a. Choosing the former space group leads to a successful solution with six atoms on the mirror plane in the fourfold special position set  $c: \pm(x, 1/4, z; 1/2 + x, 1/4, 1/2 - z)$  and four more atoms in the general set of positions:  $\pm(x, y, z; 1/2 - x, 1/2 + y, 1/2 + z; x, 1/2 - y, z; 1/2 + x, y, 1/2 - z)$ .

**Determination of Structure.**—The Patterson function calculated from the first ( $\lambda\text{Mo}$ ) data set was discouragingly featureless, consisting primarily of two positive regions at  $y = 0$  and  $1/2$ , with a negative region between (*i.e.*, it was dominated by very strong  $0k0$  reflections).

(4) J. Karle and I. L. Karle, *Acta Cryst.*, **21**, 849 (1966).

(5) R. E. Long, Ph.D. Thesis, University of California, Los Angeles, Calif., 1965.

(6) "International Tables for X-Ray Crystallography," Vol. III, The Kynoch Press, Birmingham, England, 1962, pp 202-203, 214-215.

(7) D. T. Cromer and J. T. Waber, *Acta Cryst.*, **13**, 104 (1965).

(8) D. T. Cromer, *ibid.*, **13**, 17 (1965).

(9) No significant changes in either the structural parameters or the quality of agreement were found as a result of the change in scattering factors.

TABLE I  
 FINAL POSITIONAL AND THERMAL PARAMETERS IN  $B_4F_6 \cdot PF_3$ 

Atom	<i>x</i>	<i>y</i>	<i>z</i>	$B_{11}^a$	$B_{22}$	$B_{33}$	$B_{12}$	$B_{13}$	$B_{23}$	$[\overline{U^2}]^{1/2}$
P	0.0998 (1) <sup>b</sup>	1/4 <sup>c</sup>	0.5699 (4)	5.8 (1)	6.0 (1)	8.5 (1)	0 <sup>c</sup>	0.0 (1)	0	(0.33, 0.27, 0.27) <sup>d</sup>
F1(P)	0.0497 (3)	1/4	0.7931 (10)	8.6 (3)	15.8 (5)	11.8 (4)	0	4.8 (3)	0	(0.45, 0.44, 0.25)
F2(P)	0.0524 (2)	0.1403 (3)	0.4588 (7)	7.8 (2)	9.2 (2)	17.9 (4)	-2.4 (1)	-2.7 (2)	-2.5 (2)	(0.49, 0.37, 0.25)
B(1)	0.2311 (5)	1/4	0.5805 (10)	4.9 (3)	3.2 (3)	3.7 (3)	0	0.4 (3)	0	(0.26, 0.22, 0.21)
B(2)	0.2788 (7)	1/4	0.3255 (14)	7.3 (5)	4.0 (3)	5.3 (5)	0	1.0 (4)	0	(0.31, 0.25, 0.23)
F1(2)	0.2264 (4)	1/4	0.1424 (7)	15.0 (4)	8.9 (3)	3.6 (2)	0	-1.3 (2)	0	(0.44, 0.33, 0.20)
F2(2)	0.3694 (3)	1/4	0.2902 (8)	8.9 (3)	9.7 (3)	8.6 (3)	0	4.2 (2)	0	(0.40, 0.35, 0.24)
B(3)	0.2697 (4)	0.3788 (5)	0.7122 (8)	7.8 (3)	4.2 (2)	4.4 (2)	0.0 (3)	-0.2 (2)	0.3 (2)	(0.32, 0.24, 0.23)
F1(3)	0.2131 (2)	0.4693 (3)	0.7870 (5)	12.3 (2)	4.9 (1)	7.6 (2)	1.4 (1)	0.5 (1)	-1.9 (1)	(0.40, 0.33, 0.21)
F2(3)	0.3598 (2)	0.4004 (3)	0.7500 (6)	9.3 (2)	7.0 (2)	11.3 (2)	-1.8 (2)	-3.1 (2)	-1.7 (2)	(0.41, 0.34, 0.24)

<sup>a</sup> The units are Å<sup>2</sup>. <sup>b</sup> The number in parentheses is the standard deviation in the least significant digit as derived from the least-squares matrix. <sup>c</sup> Values expressed without the use of a decimal point are fixed by symmetry. <sup>d</sup> These are the principal root-mean-square amplitudes of vibration, in order of magnitude. For orientations, see Figures 1 and 2.

Several attempts at refining various trial structures guessed at from this Patterson function met with no success whatever. We reasoned that the strong  $0k0$  reflections would arise only if some large fraction of the atoms were concentrated at or near the same  $y$  coordinate, as would be the case if the molecule were bisected by the mirror plane in Pnma. With this in mind, the Wilson-plot program was used to calculate normalized structure factor magnitudes,<sup>4</sup>  $E_h$ , for use in the statistical method of sign determination (centrosymmetric case). For this purpose, we employed Long's program<sup>5</sup> which iteratively applies the relation:  $sE_h \sim s\sum_k E_k E_{h-k}$ , where  $s$  is to be read "the sign of." After enough of the signs had been worked out by hand to yield a good starting set (of  $E$ 's) for input, a run of Long's program using 99  $E$ 's  $\geq 1.5$  gave one set of signs which was more consistent than any other and which was arrived at in the fewest passes. A Fourier synthesis using the signed  $E$ 's as coefficients gave ten largest peaks, six of them in the mirror plane, which formed the expected molecule. Least-squares refinement of isotropic phosphorus, fluorine, and boron atoms in the appropriate positions quickly reduced the  $R$  factor to 0.29, where  $R = \sum ||kF_o| - |F_c|| / \sum |kF_o|$ . It was immediately evident that the  $0k0$  reflections had given intensities which were systematically too large by factors between 3.6 and 5.2. A refinement in which the  $0k0$  reflections were given zero weight did not reduce  $R$ , but when they were omitted from the calculation of  $R$ , its value became 0.26. When all atoms were allowed anisotropic temperature factors,  $R$  fell to 0.180 on all data and 0.145 if the  $0k0$ 's were omitted. These values could not be improved upon and a rerun of Long's program with the  $0k0$  reflections omitted gave the same structure a second time.

At this time the first (Mo) data set was discarded and the second crystal and second (Cu) data set were obtained as described above. The structure found from the first data set refined to  $R = 0.217$  with isotropic temperature factors. When all atoms were allowed anisotropic temperature factors, the structure gave the final  $R$  value of 0.093 on all 703 data and this

can be reduced to 0.067 by omitting the contributions from the 100 reflections which were recorded as having zero intensity. In the last cycle of the refinement, no parameter shifted by as much as 1% of the standard deviation calculated for it from the least-squares matrix. The standard deviation of an observation of unit weight, defined as  $[\sum w(|kF_o| - |F_c|)^2 / (u - v)]^{1/2}$  where  $u$  is the number of data and  $v$  is the number of independent parameters refined, was 1.33. Tests of slightly noncentric structures in the other space group (Pn2<sub>1</sub>a) gave neither better agreement nor significant deviations from the higher symmetry. The magnitudes of the three largest peaks on a final difference Fourier were 0.50, 0.38, and 0.30 e<sup>-</sup>/Å<sup>3</sup>. The final positional and thermal parameters are presented in Table I, while Table II lists  $|F_o|$  and  $F_c$ .

### Discussion

The  $B_4F_6 \cdot PF_3$  molecule is shown in Figure 1. The duplicate atom labels are caused by the crystallographic mirror plane which bisects the molecule and contains F1(P), P, B(1), B(2), F1(2), and F2(2). The atoms F2(P), P, B(1), and B(3) all lie in another plane to within the accuracy of this determination; F1(3) and F2(3) deviate from it by only a small ( $\sim 3^\circ$ ) rotation of the  $BF_2$  group about the B-B bond. This second plane makes an angle of  $120 \pm 1^\circ$  with the mirror plane so that the molecule has approximately 3m ( $C_{3v}$ ) point symmetry, only one mirror of which is required by the crystal symmetry. The fluorines on phosphorus atoms are in a staggered configuration with respect to the  $BF_2$  groups on B(1), and the angles at B(1) are tetrahedral to within the experimental accuracy.

Distances and angles found in this structure are presented and compared with those found for related compounds in Table III. These interatomic distances must be corrected for the effect of thermal motion in order to arrive at quantities which are comparable with the results of studies by other methods (e.g., spectroscopic and electron diffraction methods). This is



TABLE III  
 DISTANCES AND ANGLES IN  $B_4F_6 \cdot PF_3$  AND COMPARISON COMPOUNDS

Atoms	Dist, Å	Comparison dist, Å	Comparison compd
B(2)-F1(2)	1.330 (10) <sup>a</sup>		
B(2)-F2(2)	1.276 (10)		
B(3)-F1(3)	1.319 (6)		
B(3)-F2(3)	1.293 (7)	1.30	BF <sub>3</sub> <sup>d</sup>
Av	1.305 ± 0.015 <sup>b</sup>	1.32 ± 0.035	B <sub>2</sub> F <sub>4</sub> <sup>e</sup>
(Thermal correction = 0.009, 0.051) <sup>c</sup>			
B(1)-B(2)	1.685 (10)		
B(1)-B(3)	1.668 (7)		
Av	1.677 ± 0.015	1.67 ± 0.045	B <sub>2</sub> F <sub>4</sub>
(Thermal correction = 0.001, 0.013)			
B(1)-P	1.825 (7)		
	1.825 ± 0.015 <sup>b</sup>	1.836 ± 0.012	H <sub>3</sub> B · PF <sub>3</sub> <sup>f</sup>
(Thermal correction = 0.005, 0.026)			
P-F1(P)	1.525 (6)		
P-F2(P)	1.496 (4)	1.535 ± 0.02	PF <sub>3</sub> <sup>g</sup>
Av	1.511 ± 0.015	1.538 ± 0.008	H <sub>3</sub> B · PF <sub>3</sub>
(Thermal correction = 0.013, 0.066)			
Intramolecular, Nonbonded Distances			
B(2)-B(3)	2.719 (9)		
B(3)-B(3)	2.725 (11)		
F1(2)-F2(2)	2.180 (7)		
F1(3)-F2(3)	2.176 (4)	2.23 ± 0.024	B <sub>2</sub> F <sub>4</sub>
F1(P)-F2(P)	2.339 (7)		
F2(P)-F2(P)	2.321 (7)		
F2(2)-F2(3)	3.217 (5)		
F2(3)-F2(3)	3.181 (7)		
F1(2)-F2(P)	3.299 (6)		
F1(3)-F1(P)	3.246 (4)		
F1(3)-F2(P)	3.210 (5)		
Intermolecular F-F Contacts <sup>h</sup>			
F2(P)-F2(3)	3.088 (5)	[3.095]	B <sub>2</sub> F <sub>4</sub>
F1(P)-F2(3)	3.092 (5)	[3.11]	B <sub>2</sub> F <sub>4</sub>
F1(2)-F1(3)	3.174 (4)	[3.125]	B <sub>2</sub> F <sub>4</sub>
F2(P)-F2(2)	3.178 (6)	[3.22]	B <sub>2</sub> F <sub>4</sub>
F2(2)-F1(3)	3.183 (3)	[3.27]	B <sub>2</sub> F <sub>4</sub>
F1(2)-F1(3)	3.209 (4)	[3.28]	B <sub>2</sub> F <sub>4</sub>
F2(P)-F2(3)	3.236 (5)	[3.28]	B <sub>2</sub> F <sub>4</sub>
F1(P)-F1(2)	3.244 (7)	[3.30]	B <sub>2</sub> F <sub>4</sub>
F1(3)-F1(3)	3.271 (2)	[3.34]	B <sub>2</sub> F <sub>4</sub>
F1(3)-F2(3)	3.292 (5)	[3.37]	B <sub>2</sub> F <sub>4</sub>
F2(P)-F2(P)	3.343 (7)	[3.45]	B <sub>2</sub> F <sub>4</sub>
F1(2)-F2(3)	3.413 (5)		
All others	>3.5		
Atoms	Angle, deg	Comparison angle, deg <sup>h</sup>	Comparison compd
F1(2)-B(2)-F2(2)	113.6 (7)		
F1(3)-B(3)-F2(3)	112.8 (5)		
Av	113.2 ± 1	[115]	B <sub>2</sub> F <sub>4</sub>
B(1)-B(2)-F1(2)	123.6 (7)		
B(1)-B(2)-F2(2)	122.8 (7)		
B(1)-B(3)-F1(3)	124.5 (5)		
B(1)-B(3)-F2(3)	122.7 (5)		
Av	123.4 ± 1	[122.5]	B <sub>2</sub> F <sub>4</sub>
B(2)-B(1)-B(3)	108.3 (4)		
B(3)-B(1)-B(3)	109.5 (5)		
B(2)-B(1)-P	111.1 (5)		
B(3)-B(1)-P	109.8 (3)		
Av	109.7 ± 1	109.5	(Tetrahedral)
B(1)-P-F1(P)	115.2 (3)		
B(1)-P-F2(P)	117.2 (2)		
Av	116.2 ± 1		
F1(P)-P-F2(P)	101.5 (2)		
F2(P)-P-F2(P)	101.8 (3)	100 ± 2	PF <sub>3</sub>
Av	101.7 ± 1	99.8 ± 1	H <sub>3</sub> B · PF <sub>3</sub>

TABLE III (Footnotes)

<sup>a</sup> The number in parentheses is the standard deviation in the least significant digit as calculated from the standard deviations of coordinates. <sup>b</sup> The standard deviations of 0.015 Å and 1° listed for average values are based upon comparisons of distances expected to be the same and the authors' past experience. They are believed to be better representations of the accuracy of these results than those calculated from the standard deviations of coordinates. <sup>c</sup> The two corrections for thermal motion given are a minimum correction and a "riding-model" correction, respectively. Both are much less than the maximum possible correction. (See text and ref 10.) <sup>d</sup> "Tables of Interatomic Distances and Configuration in Molecules and Ions," Special Publication No. 11, The Chemical Society, Burlington House, London, 1958, p M18. <sup>e</sup> L. Trefonas and W. N. Lipscomb, *J. Chem. Phys.*, **28**, 54 (1958). <sup>f</sup> R. L. Kuczkowski and D. R. Lide, Jr., *ibid.*, **46**, 357 (1967) (microwave study). <sup>g</sup> Q. Williams, J. Sheridan, and W. Gordy, *ibid.*, **20**, 164 (1952) (microwave and electron diffraction study). <sup>h</sup> Numbers in brackets are the authors' calculation from cell dimensions and positional parameters given (X-ray crystallographic study).

propeller-like configuration. The observation that each fluorine has at least two intermolecular F-F contacts shorter than any intramolecular one (except between two fluorines bonded to the same atom) shows that the fluorine contacts within the molecule are not short enough to control the configuration. The BF<sub>2</sub> orientations are evidently governed by the meshing together of fluorine atoms on adjacent molecules (see Figure 2). The existence of intermolecular F-F contacts shorter than the intramolecular ones also indicates that the B-P distance is not controlled by F-F interactions. This, and the fact that the B-P distance found here is not significantly different from that found for H<sub>3</sub>B·PF<sub>3</sub>, indicates that BF<sub>2</sub> will not only formally replace hydrogen<sup>3</sup> but is also quite similar to hydrogen in its electronic effects on the rest of the molecule.

Inspection of the magnitudes and directions of the principal axes of the thermal ellipsoids reveals that the greatest anisotropy is in the motion of the fluorine atoms and that the largest amplitudes are in directions which are more or less perpendicular to bond directions. A considerable component of this motion may consist of librations of the PF<sub>3</sub> and BF<sub>2</sub> groups about the directions of their bonds to the central boron atom, but bending vibrations also appear to be important.

**Acknowledgment.**—We thank Professor Timms for providing the samples which made this work possible and for providing them in such a convenient form. We also thank Professor Timms and Mr. Ralph Kirk for helpful discussions regarding the significance of these results.

---

CONTRIBUTION NO. 1463 FROM THE CENTRAL RESEARCH DEPARTMENT,  
E. I. DU PONT DE NEMOURS AND COMPANY, EXPERIMENTAL STATION, WILMINGTON, DELAWARE 19898

## Crystal Chemistry of Metal Dioxides with Rutile-Related Structures

By D. B. ROGERS, R. D. SHANNON, A. W. SLEIGHT, AND J. L. GILLSON

Received May 20, 1968

In order to attempt a systematic correlation of the crystal chemistries of the transition metal dioxides with rutile-related structures, single crystals were grown of the oxides MO<sub>2</sub>, where M = Mn, Mo, Ru, W, Re, Os, or Ir, and certain electrical transport and crystallographic parameters were accurately determined. Trends of these parameters within the rutile family are shown to be closely associated with variations in the occupancy of the transition metal d shells. Qualitative, one-electron energy level diagrams are discussed that appear to rationalize the electrical and crystallographic properties of these materials.

### Introduction

Many metal dioxides, particularly those of the transition metals, crystallize in structural types that are closely related to that of the rutile form of TiO<sub>2</sub> (Figure 1). The properties of rutile were extensively discussed by Grant,<sup>1</sup> and structural reviews of most of the related dioxides and of compounds possessing the similar trirutile structure have been given by

Baur<sup>2</sup> and Bayer.<sup>3</sup> The dioxides of Cr, Os, Ru, Ir, Sn, and Ta are tetragonal and isomorphous with rutile; those of V, Nb, Mo, Tc, and W adopt distorted variants of the rutile structure in which the metal atoms occur in pairs along the *c* axis of the rutile pseudocell. Most of the latter oxides are monoclinic and are characterized by a tilt of the metal atom doublets in the [100] direction of the rutile subcell. NbO<sub>2</sub>, however, is tetragonal and

(1) F. A. Grant, *Rev. Mod. Phys.*, **31**, 646 (1959).

(2) W. H. Baur, *Acta Cryst.*, **9**, 515 (1956).

(3) G. Bayer, *Ber. Deut. Keram. Ges.*, **39**, 535 (1962).